This paper is available on line at http://www.mcponline.org

Discovery of Predictive Biomarkers for Litter Size in Boar Spermatozoa*

Woo-Sung Kwon‡, Md Saidur Rahman‡, June-Sub Lee‡, Sung-Jae Yoon‡, Yoo-Jin Park‡, and Myung-Geol Pang‡§

Conventional semen analysis has been used for prognosis and diagnosis of male fertility. Although this tool is essential for providing initial quantitative information about semen, it remains a subject of debate. Therefore, development of new methods for the prognosis and diagnosis of male fertility should be seriously considered for animal species of economic importance as well as for humans. In the present study, we applied a comprehensive proteomic approach to identify global protein biomarkers in boar spermatozoa in order to increase the precision of male fertility prognoses and diagnoses. We determined that L-amino acid oxidase, mitochondrial malate dehydrogenase 2, NAD (MDH2), cytosolic 5′-nucleotidase 1B, lysozyme-like protein 4, and calmodulin (CALM) were significantly and abundantly expressed in high-litter size spermatozoa. We also found that equatorin, spermadhesin AWN, triosephosphate isomerase (TPI), Ras-related protein Rab-2A (RAB2A), spermadhesin AQN-3, and NADH dehydrogenase [ubiquinone] iron-sulfur protein 2 (NDUFS2) were significantly and abundantly expressed in low-litter size spermatozoa (>3-fold). Moreover, RAB2A, TPI, and NDUFS2 were negatively correlated with litter size, whereas CALM and MDH2 were positively correlated. This study provides novel biomarkers for the prediction of male fertility. To the best of our knowledge, this is the first work that shows significantly increased litter size using male fertility biomarkers in a field trial. Moreover, these protein markers may provide new developmental tools for the selection of superior sires as well as for the prognosis and diagnosis of male fertility. ***Molecular & Cellular Proteomics 14: 10.1074/mcp. M114.045369, 1230–1240, 2015.***

Prognosis and diagnosis of male fertility is a major concern in both animals and humans worldwide. In humans, about half of the fertility problems arise because of male factors. In addition, 50% of breeding system failures that are contributed by the sire lead to huge economic drawbacks in the animal industry (1–5). Therefore, the development of new methods is needed to ensure more accurate prognosis and diagnosis of male fertility.

Worldwide, artificial insemination (AI)[1] has been extensively performed in animal industries. Recent data revealed that more than 90% of the sows in Europe and the United States have been bred using AI during last three decades (6). The AI system sufficiently contributes to the achievement of high performance swine production through the selection of quality semen. Moreover, AI has been implemented extensively in swine industries for genetic up-grading (7, 8). However, the selection of high quality semen still depends on conventional sperm analyses such as the analysis of sperm morphology (9), motility (10), and sperm penetration assays (11, 12). Although these tests are commonly used to evaluate the male factor of fertility/infertility, the clinical value is still debated (13). Therefore, to evaluate the limits of conventional sperm analyses, the development of new methods to assess sperm function and fertility should be seriously considered for animal species of economic importance as well as for humans. Additionally, it is important to note that the optimization of sperm production will be possible when the methods to choose superior sires with greater efficiency become available. In this regard, the identification of global protein biomarkers using comprehensive proteomic tools represents a new method on the horizon that may facilitate the prediction of superior sires.

Recently, several studies have reported that proteomics is an effective tool that has the potential to transform our understanding of spermatozoa (14–16) by acquiring new biomarkers of male infertility and/or fertility. In addition, the de-

From the ‡Department of Animal Science & Technology, Chung-Ang University, Anseong, Gyeonggi-do 456-756, Republic of Korea.

Received October 1, 2014, and in revised form, February 16, 2015
Published, MCP Papers in Press February 19, 2015, DOI 10.1074/mcp.M114.045369

Author contributions: W.K. and M.P. designed research; W.K., M.R., J.L., S.Y., Y.P., and M.P. performed research; W.K., M.R., J.L., S.Y., Y.P., and M.P. analyzed data; W.K., M.R., and M.P. wrote the paper.

[1] The abbreviations used are: AI, artificial insemination; CASA, computer-assisted sperm analysis; ELISA, enzyme-linked immunosorbent assay; VCL, curvilinear velocity; VSL, straight-line velocity; VAP, average path velocity; ALH, amplitude of head lateral displacement; H33258/CTC, combined hoechst 33258/chlortetracycline fluorescence assessment; ESI, nano-electrospray ionization; CALM, calmodulin; EQTN, equatorin; NT5C1B, cytosolic 5′-nucleotidase 1B; RAB2A, Ras-related protein Rab-2A; NDUFS2, NADH dehydrogenase [ubiquinone] iron-sulfur protein 2; TPI, triosephosphate isomerase; AWN, spermadhesin AWN; LYZL4, lysozyme-like protein 4; AQN-3, spermadhesin AQN-3; LAAO, L-amino-acid oxidase; MDH2, mitochondrial malate dehydrogenase 2.

velopment of mass spectrometry (MS) allows the potential identification of sperm proteins (17, 18). In fact, increased knowledge of the sperm proteome allows us to identify new molecular markers.

In this study, we used high- and low-litter size boar spermatozoa to develop suitable biomarkers. First, sperm motility (%), motion characteristics, and capacitation status were evaluated by computer-assisted sperm analysis (CASA) and combined Hoechst 33258/chlortetracycline fluorescence assessment. Second, to find deferentially expressed proteins (>threefold) between high- and low-litter size boar spermatozoa, a 2-DE proteomic approach was applied following the identification of proteins by ESI-MS/MS and a MASCOT search. The 2-DE results were confirmed by a Western blot analysis that was performed with five commercially available antibodies. Third, to validate discovered markers for male fertility prediction, the expression levels of five proteins from 20 randomly selected boar spermatozoa with broad fertility ranges (*i.e.* litter size) were analyzed by enzyme-linked immunosorbent assay (ELISA), and the relationship between protein expression and male fertility was determined. Moreover, to represent the entire proteomic event, biological functions and interactions of the deferentially expressed proteins were schematized by a signaling pathway.

EXPERIMENTAL PROCEDURES

All procedures were performed according to guidelines for the ethical treatment of animals, and were approved by the Institutional Animal Care and Use Committee of Chung-Ang University.

Sample Preparation—Landrace semen samples were collected from grand-grandparents farm of Sunjin Co. (Danyang, Korea). The entire ejaculate from AI stud boar was collected by gloved-hand technique (19). The semen was diluted to a density of 30×10^6 sperm cells/ml in 100 ml of commercial extender (Beltsville thawing solution). Extended semen was cooled down and stored in semen storage at 17 °C. Finally, semen samples from 18 boars were considered to inseminate 686 sows by AI (average insemination = 38.11 ± 3.24 times). Litter size was scored by total live pups from individual boar (total pups/total breeding, average litter size = 10.95 ± 0.16). To eliminate fertility variation, only parity 2–8 (multiparous) fertility data was included because of primiparous (first parity) sow is sensitive to several environmental factors (20). Semen samples were then divided into two parts based on litter size such as high- (12.3 ± 0.07) and low-litter size (10.2 ± 0.09) ($p < 0.01$; Fig. 1). Both samples were randomly divided into three groups ($n = 3$) for experimental replication. To rule out individual variation, each group was pooled, and pooled samples were washed at 500 × *g* for 20 min with a discontinuous (70% [v/v] and 35% [v/v]) Percoll gradient (Sigma, St Louis, MO) to remove seminal plasma and dead spermatozoa (21).

Computer-assisted Sperm Analysis (CASA)—Sperm motility (%) and motion kinematics were analyzed by a CASA system (SAIS Plus version 10.1, Medical Supply, Seoul, Korea) as previously described (22–24). Briefly, a 10 μl sample was placed in a Makler chamber (Makler, Haifa, Israel). The filled chamber was then placed on a 37 °C heated stage. Using a 10× objective in-phase contrast mode, the image was relayed, digitized, and analyzed by SAIS. The movement of at least 250 sperm cells was recorded for each sample from random fields (> 5). With respect to the motility setting parameters, objects with a curvilinear velocity (VCL) more than 10 μm/s were considered motile. Motility (%) and five motion kinematics parameters (*i.e.* curvilinear velocity (VCL, μm/s), straight-line velocity (VSL, μm/s), average path velocity (VAP, μm/s), and mean amplitude of head lateral displacement (ALH, μm)) were analyzed.

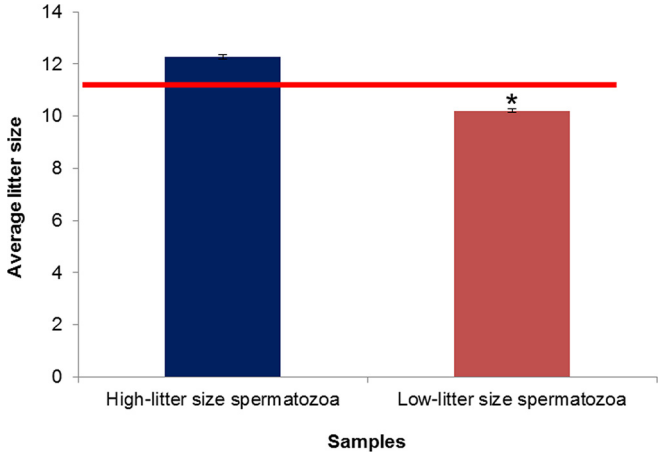

FIG. 1. **The average litter size of high- and low-litter size spermatozoa.** The data represent the mean ± S.E., $n = 3$. The red line indicates average litter size of 18 boars. *Significantly different between high- and low-litter size spermatozoa ($p < 0.01$).

Combined Hoechst 33258/Chlortetracycline Fluorescence Assessment of Capacitation Status (H33258/CTC)—To determine capacitation status, a dual staining method was performed as described previously with modification (22–25). Briefly, 135 μl of treated spermatozoa were added to 15 μl of H33258 solution (10 μg H33258/ml DPBS) and incubated for 5 min at room temperature (RT). Excess dye was removed by layering the mixture over 250 μl of 2% (w/v) polyvinylpyrrolidone in DPBS. After centrifuging at 500 × *g* for 5 min, the supernatant was discarded and the pellet was resuspended in 100 μl of DPBS and 100 μl of a freshly prepared chlortetracycline fluorescence (CTC) solution (750 mM CTC in 5 μl buffer: 20 mM Tris, 130 mM NaCl, and 5 mM cysteine, pH 7.4). Samples were observed with a Microphot-FXA microscope (Nikon) under epifluorescence illumination using ultraviolet BP 340–380/LP 425 and BP 450–490/LP 515 excitation/emission filters for H33258 and CTC, respectively. The spermatozoa were classified as live noncapacitated (F, bright green fluorescence distributed uniformly over the entire sperm head, with or without a stronger fluorescent line at the equatorial segment), live capacitated (B, green fluorescence over the acrosomal region and a dark postacrosome), or live acrosome reacted (AR, sperm showing a mottled green fluorescence over the head, green fluorescence only in the postacrosomal region, or no fluorescence over the head) (22–25). Two slides per sample were evaluated with at least 400 spermatozoa per slide.

2-DE and Gel Image Analysis—Spermatozoa (50×10^6/ml) were incubated for protein extraction in rehydration buffer containing 7 M urea (Sigma), 2 M thiourea (Sigma), 4% (w/v) 3-[(3-cholamidopropyl) dimethylamonio]-1-propanesulfonate (USB), 0.05% (v/v) Triton X-100 (Sigma), 1% (w/v) octyl β-D-glucopyranoside, 24 μM PMSF (Sigma), 1% (w/v) dithiothreitol (DTT, Sigma), 0.5% (v/v) IPG Buffer, and 0.002% (w/v) bromphenol blue at 4 °C for 1 h. Then, 250 μg of solubilized protein from the sperm cells in 450 μl of rehydration buffer were placed in a rehydration tray with 24-cm NL Immobiline DryStrips (pH 3–11; Amersham Biosciences) for 12 h at 4 °C. First-dimension electrophoresis was performed using an IPGphor isoelectric focusing apparatus, and then the strips were focused at 100 V for 1 h, 200 V for 1 h, 500 V for 1 h, 1000 V for 1 h, 5000 V for 1.5 h, 8000 V for 1.5 h, and 8000–90,000 V for 1 h. After isoelectrofocusing, the strips were

equilibrated with equilibration buffer A containing 6 M urea, 75 mM Tris-HCl (pH 8.8), 30% (v/v) glycerol, 2% (w/v) SDS, 0.002% (w/v) bromphenol blue, and 2% (w/v) DTT for 15 min at RT. The strips were equilibrated a second time with equilibration buffer B (equilibration buffer A with 2.5% (w/v) iodoacetamide (Sigma), but without DTT) for 15 min at RT. Second-dimension electrophoresis (2-DE) was conducted with 12.5% (w/v) SDS-PAGE gels with the strips at 100 V for 1 h and 500 V until the bromphenol blue front began to migrate off of the lower end of the gels. The gels were silver-stained for visualization of proteins in gels (4, 16) following the manufacturer instructions (Amersham Biosciences, Piscataway, NJ). Finally, the gels were then scanned using a high-resolution GS-800 calibrated scanner (Bio-Rad), and detected spots were matched and analyzed by comparing them with high- and low-litter size spermatozoa gels using PDQuest 8.0 software (Bio-Rad). The low-fertility spermatozoa gel was used as a control. Finally, the density of the spots was calculated and normalized as the ratio of high-/low-litter size per spermatozoa gel.

Protein Identification—

In-gel Digestion—The proteins were subjected to in-gel trypsin digestion. Excised gel spots were destained with 100 μl of destaining solution (30 mM potassium ferricyanide, 100 mM sodium thiosulfate) while shaking for 5 min. After removing the solution, the gel spots were incubated in 200 mM ammonium bicarbonate for 20 min. The gel pieces were dehydrated with 100 μl of acetonitrile and dried in a vacuum centrifuge. The above procedure was repeated three times. The dried gel pieces were rehydrated with 20 μl of 50 mM ammonium bicarbonate containing 0.2 μg modified trypsin (Promega, Fitchburg, WI) for 45 min on ice. After removing the solution, 30 μl of 50 mM ammonium bicarbonate were added. The digestion was performed overnight at 37 °C. The peptide solution was desalted using a C18 nano-column (homemade).

Desalting and Concentration—Custom-made chromatographic columns were used for desalting and concentrating the peptide mixture prior to mass spectrometric analysis. A column consisting of 100–300 ml of Poros reverse phase R2 material (20–30 μm bead size, Perseptive Biosystems) was packed into a constricted GELoader tip (Eppendorf, Hamburg, Germany). A 10 ml syringe was used to force liquid through the column by applying gentle air pressure. Thirty microliters of the peptide mixture from the digestion supernatant were diluted in 30 μl of 5% formic acid, loaded onto the column, and washed with 30 μl of 5% formic acid. For tandem mass spectrometry (MS/MS) analyses, the peptides were eluted with a solution of 1.5 μl 50% methanol, 49% H_2O, 1% formic acid directly into a precoated borosilicate nano-electrospray needle (EconoTipTM).

ESI-MS/MS—An MS/MS analysis of the peptides that were generated by in-gel digestion was performed by using a nano-electrospray ionization (ESI) on a Q-TOF2 mass spectrometer (AB Sciex Instruments). The source temperature was RT. A potential of 1 kV was applied to precoated borosilicate nano-electrospray needles (EconoTip TM, New Objective, Woburn, MA) in the ion source, combined with a nitrogen back-pressure of 0–5 psi to produce a stable flow rate (10–30 ml/min). The cone voltage was 40 V. The quadrupole analyzer was used to select precursor ions for fragmentation in the hexapole collision cell. The collision gas was argon at a pressure of $6^{-7} \times 10^{-5}$ mbar and the collision energy was 25–40 V. Product ions were analyzed using an orthogonal TOF analyzer that was fitted with a reflector, which is a microchannel plate detector and a time-to-digital converter. The data were processed using a peptide sequence system.

Database Searching—The MS/MS ion search was assigned as the ion search option in the MASCOT software (Matrix Science). Peptide fragment files were obtained from the peptide peaks in the ESI-MS/MS results. Trypsin was selected as the enzyme with one potentially missed cleavage site, and ESI-QTOF was selected as the instrument type. The peptide fragment files were searched based on the database using the MASCOT (v2.4, Matrix Science) and FASTA search engine, and the search was limited to *Sus scrofa* taxonomy in NCBInr, UniprotKB/TrEMBL and UniprotKB/Swissprot database. Oxidized methionine was set as a variable modification, and carbamidomethylated cysteine was set as a fixed modification. The mass tolerance was set at $\pm$ 1.0 and $\pm$ 0.6 Da for the peptides and fragments, respectively. High scoring peptides corresponded to those that were above the default significance threshold in MASCOT ($p < 0.05$, peptide score >35).

Western Blotting—To confirm the 2-DE results, Western blotting bands that were visualized using anti-Ras-related protein Rab-2A (RAB2A), anti-triosephosphate isomerase (TPI), anti-NADH dehydrogenase [ubiquinone] iron-sulfur protein 2 (NDUFS2), anti-calmodulin (CALM), and anti- mitochondrial malate dehydrogenase 2, and NAD (MDH2) antibodies were quantified for three individual high- and low-litter size spermatozoa. Western blotting was performed as previously described (20–22) with modification. The samples were washed twice with DPBS and centrifuged at 10,000 $\times$ *g* for 5 min. After this, the pellets were resuspended and incubated with sample buffer containing 5% 2-mercaptoethanol for 10 min at RT. After incubation, the insoluble fractions were separated by centrifugation at 10,000 $\times$ *g* for 10 min. The samples were subjected to SDS-polyacrylamide gel electrophoresis using a 12% mini-gel system (Amersham Biosciences), and the separated proteins were transferred to apolyvinylidene fluoride membranes (Amersham Biosciences). The membranes were blocked with 3% blocking agent (Amersham Biosciences) for 1 h at RT. RAB2A, TPI, NDUFS2, CALM, and MDH2 from high- and low-litter size spermatozoa were immunodetected using anti-RAB2A and anti-CALM mouse monoclonal antibodies, anti-TPI and anti-MDH2 rabbit polyclonal antibodies, and anti-NDUFS2 goat polyclonal antibody (Amersham Biosciences) that had been diluted with blocking solution (1:1000) for 2 h at RT. The membranes were then incubated with horse radish peroxidase (HRP) conjugated anti-mouse, antirabbit, and antigoat IgG (Abcam, Cambridge, UK) that had been diluted with blocking solution (1:3000) for 2 h at RT. α-tubulin was detected by conducting incubation with a monoclonal anti-α-tubulin mouse antibody (Abcam) that had been diluted with blocking solution (1:10,000) for 2 h at RT. In addition, membranes were incubated with an HRP conjugated goat anti-mouse IgG (Abcam) that had been diluted with blocking solution (1:10,000) for 1 h at RT. The proteins on the membranes were detected with an enhanced chemiluminescence (ECL) technique using ECL reagents. All of the bands were scanned with a GS-800 calibrated imaging densitometer (Bio-Rad), and were analyzed with Quantity One (Bio-Rad). Lastly, the signal intensity ratios of the bands were calculated for RAB2A, TPI, NDUFS2, CALM, and MDH2/α-tubulin.

Enzyme-linked Immunosorbent Assay (ELISA)—To determine correlation between RAB2A, TPI, NDUFS2, CALM, MDH2 and litter size in boars, an ELISA was performed with spermatozoa from 20 individual boars. Spermatozoa samples (50 $\times$ 10^6/ml) for protein extractions were incubated in rehydration buffer containing 7 M urea (Sigma), 2 M thiourea (Sigma), 4% (w/v) 3-[(3-cholamidopropyl) dimethylamonio]-1-propanesulfonate (USB), 0.05% (v/v) Triton X-100 (Sigma), 1% (w/v) octyl β-D-glucopyranoside, 24 μM PMSF (Sigma), 1% (w/v) dithiothreitol (DTT, Sigma), and 0.002% (w/v) bromphenol blue at 4 °C for 1 h. Solubilized proteins (50 μg/well) were coated on Immuno 96-well plates, and were incubated overnight at 4 °C. The plates were then blocked with blocking solution (5% [w/v] BSA in DPBS containing of 0.5% Tween-20 [PBST]) for 90 min at 37 °C. After blocking, the plates were incubated with anti-RAB2A and anti-CALM mouse monoclonal antibodies, anti-TPI and anti-MDH2 rabbit polyclonal antibodies, and an anti-NDUFS2 goat polyclonal antibody (Amersham Biosciences) that had been diluted with blocking solution (1:5000) for 90 min at 37 °C. Then, the plates were incubated with a horseradish peroxidase

(HRP) conjugated anti-mouse, anti-rabbit, and anti-goat IgG (Abcam) that had been diluted with blocking solution (1:5000) for 90 min at 37 °C. To activate peroxidase, the plates were incubated with TMB solution (Sigma) for 15 min at RT, and the reaction was stopped with 1N sulfuric acid. Finally, the signal was measured at 450 nm using a microplate reader (Gemini Em, Molecular Devices Corporation).

Quality Assessment of Parameters—Four key parameters were used in the screening tests: sensitivity, specificity, positive predictive value, and negative predictive value (11, 12, 26). Sensitivity is defined as the percentage of boars that will be correctly identified by the test based on litter size. Specificity is defined as the percentage of boars that will test truly negative. The positive predictive value is defined as the percentage of boars that test positive, but actually have a litter size ≥ 11 or < 11. The negative predictive value is defined as the percentage of boars that test negative, but actually have a litter size of ≥ 11 or < 11.

Signaling Pathway—To visualize the biological functions and signaling pathways between the differentially expressed proteins, the Pathway Studio program (v 9.0, Aridane Genomics, Rockville, MD) was used.

Statistical Analysis—The data were analyzed in SPSS (v. 18.0; Chicago, IL). Pearson correlation coefficients were calculated to determine the association between litter size and the expression levels of RAB2A, TPI, NDUFS2, CALM, and MDH2. Receiver-operating curves (ROCs) were used to assess the utility of individual analyzed parameters as a means of identifying litter size ≥ 11 or < 11 (based on average litter size). The cut-off value was calculated by ROCs, and it was determined in relation to the point of maximized specificity and sensitivity (11, 12, 26). Student's two-tailed *t* test was used to compare protein expression levels and predicted litter size by ROCs. $p < 0.05$ was considered significantly different. All data are expressed as mean ± S.E.

RESULTS

Sperm Motility, Motion Kinematics, and Capacitation Status in High- and Low-litter Size Spermatozoa—To evaluate sperm motion characteristics and capacitation status parameters in high- and low-litter size spermatozoa, CASA and H33258/CTC staining were performed. Motility, motion kinematics, and capacitation status parameters from low-litter size spermatozoa were as follows: motility (MOT) = 88.94 ± 1.30%, VCL = 152.92 ± 10.40 μm/s, VSL = 76.64 ± 7.61 μm/s, VAP = 88.71 ± 6.11 μm/s, ALH = 6.93 ± 0.40 μm, AR = 1.12 ± 0.41%, F = 91.55 ± 3.92%, and B = 7.33 ± 3.72%. In addition, motility, motion kinematics, and capacitation status parameters from high-litter size spermatozoa were as follows: MOT = 91.43 ± 2.55%, VCL = 159.10 ± 9.89 μm/s, VSL = 74.80 ± 5.80 μm/s, VAP = 87.53 ± 10.47 μm/s, ALH = 7.11 ± 0.43 μm, AR = 2.10 ± 1.13%, F = 87.14 ± 0.63%, and B = 10.75 ± 0.97% (Table I). However, none of parameters differed significantly between the two groups.

Proteomic Analysis and Identification of Fertility-related Proteins—Identification of the differentially expressed proteins related to fertility in high- and low-litter size spermatozoa by 2-DE analysis was conducted using 24-cm NL Immobiline DryStrips (pH 3–11). The spots were stained using silver staining, and were analyzed using an image analyzer (Fig. 2). Moreover, the spots were normalized as the ratio of high-/low-litter size per spermatozoa gel. Eleven spots exhibiting significantly different expression levels between high- and low-litter size spermatozoa (>threefold; $p < 0.05$; Fig. 2 and 3) were screened and detected. The differentially expressed spots (>threefold) were identified by performing an MS/MS ion search using MASCOT software (Matrix Science, Boston, MA). The identified spots were CALM, equatorin (EQTN), cytosolic 5′-nucleotidase 1B (NT5C1B), RAB2A, NDUFS2, TPI, spermadhesin AWN (AWN), lysozyme-like protein 4 (LYZL4), spermadhesin AQN-3 (AQN-3), L-amino acid oxidase (LAAO), and MDH2 (Table II). Additionally, EQTN, AWN, TPI, RAB2A, AQN-3, and NDUFS2 were significantly and abundantly expressed in low-litter size spermatozoa as compared with high-litter size spermatozoa (>threefold; $p < 0.05$; Fig. 3*A*). However, LAAO, MDH2, NT5C1B, LYZL4, and CALM were significantly and abundantly expressed in high-litter size spermatozoa as compared with low-litter size spermatozoa (>threefold; $p < 0.05$; Fig. 3*B*).

TABLE I

Sperm motility, motion kinematics, and capacitation status in low- and high-litter size spermatozoa. Sperm motility, motion kinematics and capacitation status are presented as mean ± S.E., n = 3. MOT = motility (%); VCL = curvilinear velocity (μm/s); VSL = straight-line velocity (μm/s); VAP = average path velocity (μm/s); ALH = mean amplitude of head lateral displacement (μm); AR = live acrosome reacted pattern (%); F = live non-capacitated pattern (%); B = live capacitated pattern (%)

Sperm motility, motion kinematics, and capacitation status	High-litter size spermatozoa	Low-litter size spermatozoa
MOT (%)	91.43 ± 2.55	88.94 ± 1.30
VCL (μm/s)	159.10 ± 9.89	152.92 ± 10.40
VSL (μm/s)	74.80 ± 5.80	76.64 ± 7.61
VAP (μm/s)	87.53 ± 10.47	88.71 ± 6.11
ALH (μm)	7.11 ± 0.43	6.93 ± 0.40
AR (%)	2.10 ± 1.13	1.12 ± 0.41
F (%)	87.14 ± 0.63	91.55 ± 3.92
B (%)	10.75 ± 0.97	7.33 ± 3.72

Protein Confirmation by Western Blotting—To validate the 2-DE results, the differentially expressed proteins were further examined via a Western blot analysis using commercially available antibodies. RAB2A, TPI, NDUFS2, CALM, and MDH2 were detected at 24 kDa, 27 kDa, 49 kDa, 17 kDa, and 33 kDa, respectively. These protein expression patterns were similar to the 2-DE results (Fig. 4). The density of RAB2A, TPI, and NDUFS2 were significantly more abundant in low-litter size spermatozoa as compared with high-litter size spermatozoa ($p < 0.05$), and CALM and MDH2 were significantly more abundant in high-litter size spermatozoa as compared with low-litter size spermatozoa ($p < 0.05$, Fig. 4).

Correlations Between Litter Size and the Expression Levels of RAB2A, TPI, NDUFS2, CALM, and MDH2—To validate discovered markers for male fertility prediction, the expression levels of five proteins (RAB2A, TPI, NDUFS2, CALM, and MDH2) from 20 randomly selected boar spermatozoa with broad fertility ranges (*i.e.* litter size) were analyzed by ELISA.

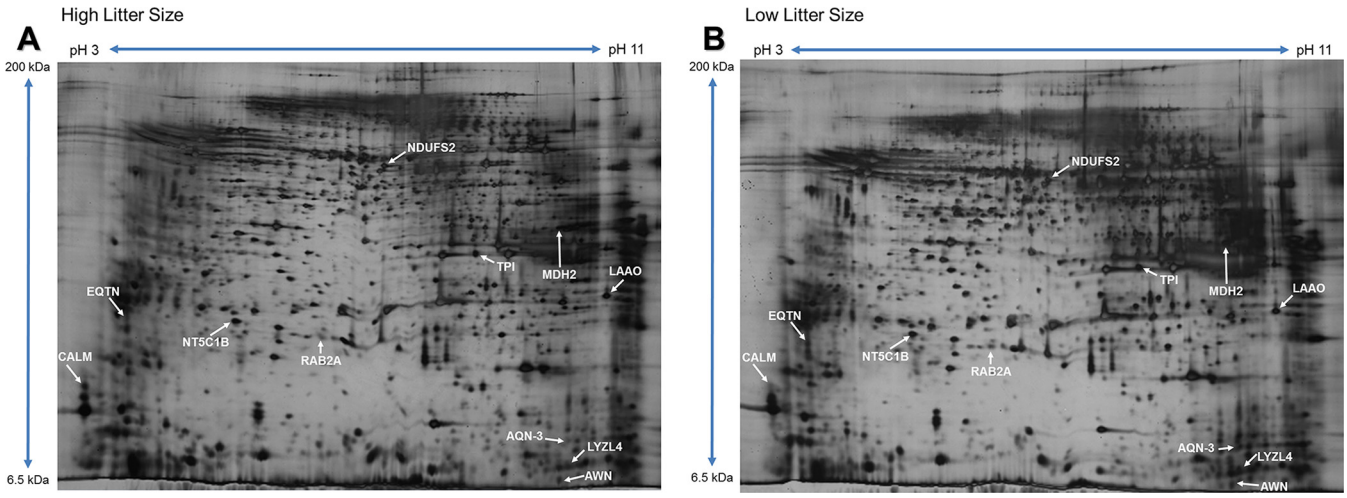

FIG. 2. **Separation of proteins by 2-DE.** 2-DE gels were stained with silver nitrate and analyzed using PDQuest 8.0 software. *A,* Protein spots from high-litter size spermatozoa. *B,* Protein spots from low-litter size spermatozoa.

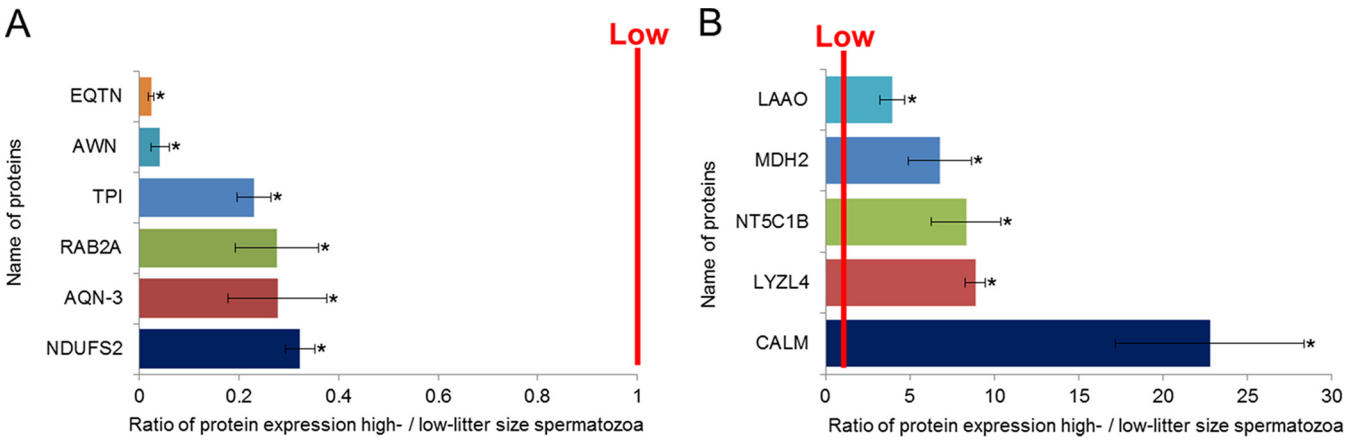

FIG. 3. **Comparison of proteins from high- and low-litter size spermatozoa.** Differentially expressed (>3-fold) proteins were determined by comparing high- and low-litter size spermatozoa ($^{*}p < 0.05$). The line indicates the landmark of low-litter size spermatozoa. *A,* Six proteins were significantly and abundantly expressed in low-litter size spermatozoa. *B,* Five proteins were significantly and abundantly expressed in high-litter size spermatozoa. The data represent the mean ± S.E., $n = 3$.

To determine the correlations between litter size and the expression levels of RAB2A, TPI, NDUFS2, CALM, and MDH2, Pearson correlation coefficients were calculated. RAB2A, TPI, and NDUFS2 were negatively correlated with litter size ($r = -0.624$, -0.797, and -0.655, respectively; $p < 0.01$, Table III), and CALM and MDH2 were positively correlated with litter size ($r = 0.665$ and 0.638, respectively; $p < 0.01$, Table III).

Quality Assessment of Parameters—To determine the cut-off value for litter size, an ROC curve was used. According to this curve, the cut-off expression values of RAB2A (0.118), TPI (1.115), NDUFS2 (0.930), CALM (0.275), and MDH2 (0.925) corresponded to the maximized sensitivity and specificity. Therefore, these values were established as the lower limits (Table IV). In terms of the expression level of RAB2A, the sensitivity, specificity, negative predictive value, and positive predictive value were 90.91%, 44.44%, 80.00%, and 66.67%, respectively. The overall accuracy of the prediction of eleven litters was 70.00% (Table IV). The low litter size of boars above the cut-off (> 0.118) was 10.54 piglets, whereas the average litter size of boars below the cut-off (≤ 0.118) was 11.31 piglets ($p < 0.05$, Fig. 5*A*). The sensitivity, specificity, negative predictive value, and positive predictive value of TPI were 72.73%, 44.44%, 57.14%, and 61.54%, respectively. The overall accuracy of the prediction of litter size ≥ 11 was 60.00% (Table IV). The average litter size of boars above the cut-off (> 1.115) was 10.70 piglets, and the average litter size of boars below the cut-off (≤ 1.115) was 11.39 piglets ($p < 0.05$, Fig. 5*B*). Regarding NDUFS2, the sensitivity, specificity, negative predictive value, and positive predictive values were 90.91%, 44.44%, 80.00%, and 66.67%, respectively. The overall accuracy of the prediction of litter size ≥11 was 70.00% (Table IV). The average litter size of boars above the cut-off (> 0.930) was 10.54 piglets, whereas the average litter size of boars below the cut-off (≤ 0.930) was 11.31 piglets ($p < 0.05$, Fig. 5*C*). The sensitivity, specificity, negative predictive value, and positive predictive

TABLE II
Differentially expressed (> 3-fold) proteins identified by ESI-MS/MS

gi no.	Symbol	Protein description	Peptide sequence	Mascot score[a]
gi 2654179	CALM	Calmodulin	G.NGYISAAELR.H	61
gi 31124567	EQTN	Equatorin	R.ATTDLNFSLR.N	60
gi 335285849	NT5C1B	Cytosolic 5′-nucleotidase 1B	R.LINSVNHYGLLIDR.F R.VAFDGDACLFSDESDHVTK.E	59
gi 31125379	RAB2A	Ras-related protein Rab-2A	K.LQIWDTAGQESFR.S	55
gi 54582230	NDUFS2	NADH dehydrogenase [ubiquinone] iron-sulfur protein 2	K.LLNIQPPPR.A R.LVMELSGEMVR.K R.IDELEEMLTNNR.I K.GEFGVYLVSDGSSRPYR.C K.LYTEGYQVPPGATYTAIEAPK.G	139
gi 80971510	TPI	Triosephosphate isomerase	K.DLGATWVVLGHSER.R K.VVLAYEPVWAIGTGK.T	88
gi 248304	AWN	Spermadhesin AWN	K.ICGGISLVFR.S K.EYVELLDGPPGSEIIGK.I	90
gi 31126871	LYZL4	Lysozyme-like protein 4	K.FNPTAVYDNLR.G R.GDYTGYGLFQIR.N	73
gi 114083	AQN-3	Spermadhesin AQN-3	F.VYQSSHNVATVK.Y	56
gi 54583217	LAAO	L-amino-acid oxidase	R.ITFTPPLTR.R R.LALNDVAALHGPIVYR.L K.ALTADAVLLTVSGPALQR.I R.IYFAGEHTAFPHGWVETAVK.S	217
gi 164541	MDH2	Mitochondrial malate dehydrogenase 2, NAD	K.VDFPQDQLSTLTGR.I	59

[a] MASCOT score is −10 log (*P), where P* is the probability that the observed match is a random event. Individual scores > 50 indicate identity or extensive homology ($p < 0.05$).

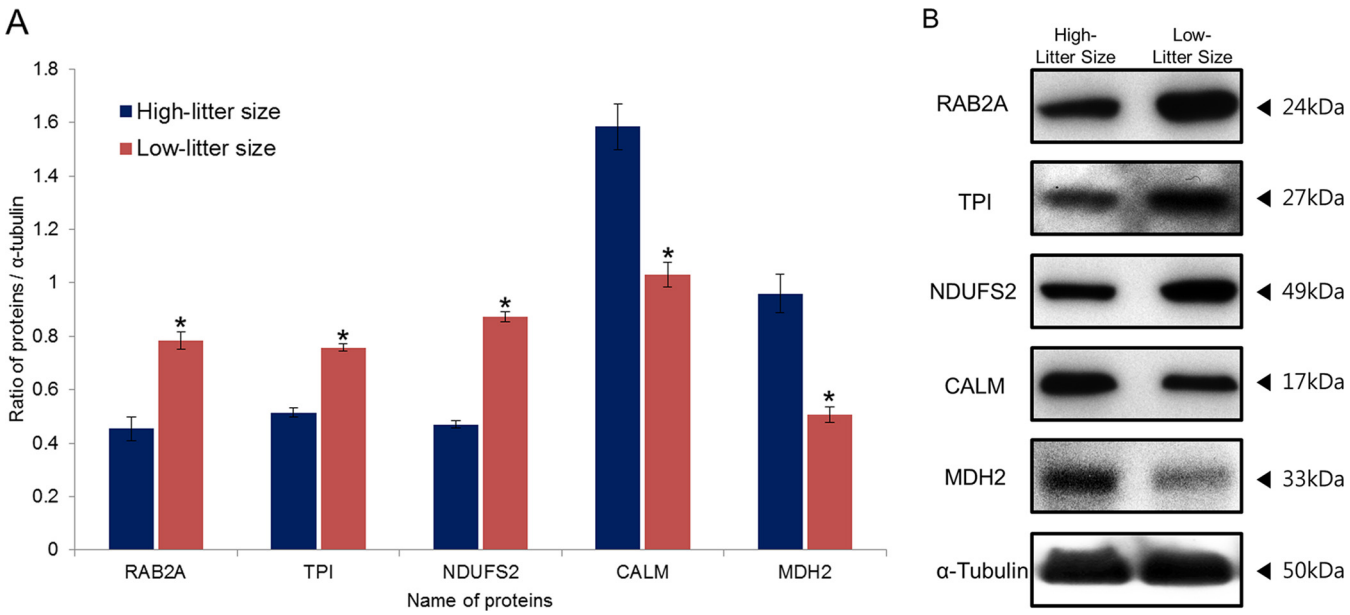

FIG. 4. **Expression of RAB2A, TPI, NDUFS2, CALM, and MDH2 in high- and low-litter size spermatozoa.** *A,* Ratios of RAB2A, TPI, NDUFS2, CALM, and MDH2 [optical density (OD × mm)/α-tubulin (OD × mm)] in high- and low-litter size spermatozoa. Data represent mean ± S.E., $n = 3$. Protein expression ratios denoted with an asterisk were significantly different (*$p < 0.05$). *B,* RAB2A, TPI, NDUFS2, CALM, and MDH2 were probed with anti-RAB2A, anti-TPI, anti-NDUFS2, anti-CALM, and anti-MDH2 antibodies.

value of CALM were 81.82%, 88.89%, 80.00%, and 90.00%, respectively. The overall accuracy of the prediction of litter size ≥ 11 was 85.00% (Table IV). The average litter size of boars below the cut-off (< 0.275) was 10.77 piglets, and the average litter size of boars above the cut-off (≥ 0.275) was 11.46 piglets ($p < 0.05$, Fig. 5*D*). Lastly, regarding MDH2, the sensitivity, specificity, negative predictive value, and positive predictive values were 90.91%, 66.67%, 85.71%, and 76.92%, respec-

TABLE III
Correlations between litter size and expression level of RAB2A, TPI, NDUFS2, CALM, and MDH2 in boar spermatozoa

	Litter size	RAB2A	TPI	NDUFS2	CALM	MDH2
Litter Size	1	−0.624**	−0.797**	−0.655**	0.665**	0.638**
RAB2A			0.468*	0.615**	−0.286	−0.360
TPI				0.465*	−0.422	−0.587**
NDUFS2					−0.488*	−0.256
CALM						0.623**
MDH2						1

* $p < 0.05$. ** $p < 0.01$.

TABLE IV
Correlation between expression level of RAB2A, TPI, NDUFS2, CALM, MDH2 and litter size

	Sensitivity (%)	Specificity (%)	Negative predictive value (%)	Positive predictive value (%)	Overall accuracy (%)
RAB2A	90.91	44.44	80.00	66.67	70.00
TPI	72.73	44.44	57.14	61.54	60.00
NDUFS2	90.91	44.44	80.00	66.67	70.00
CALM	81.82	88.89	80.00	90.00	85.00
MDH2	90.91	66.67	85.71	76.92	80.00

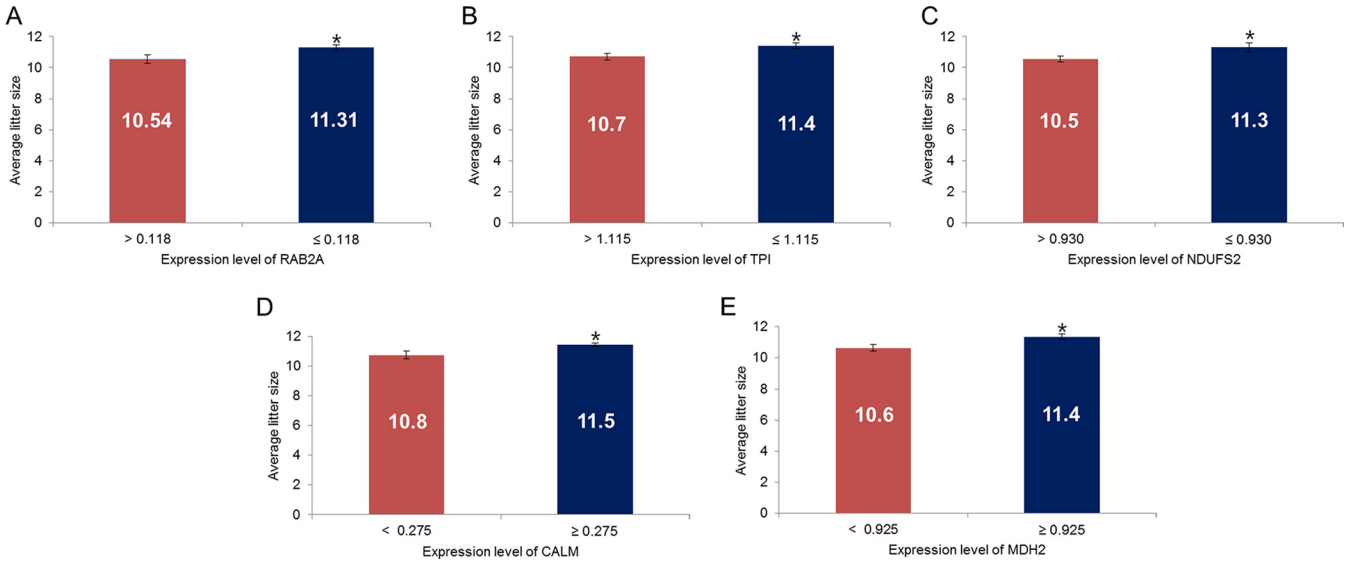

FIG. 5. **Average litter size using expression levels of RAB2A, TPI, NDUFS2, CALM, and MDH2 in spermatozoa.** *A,* Average litter size by percentage of RAB2A expression level. *B,* Average litter size by percentage of TPI expression level. *C,* Average litter size by percentage of NDUFS2 expression level. *D,* Average litter size by percentage of CALM expression level. *E,* Average litter size by percentage of MDH2 expression level.

tively. The overall accuracy of the prediction of litter size ≥11 was 80.00% (Table IV). The average litter size of boars below the cut-off (< 0.925) was 10.64 piglets, whereas the average litter size of boars above the cut-off (≥ 0.925) was 11.37 piglets ($p < 0.05$, Fig. 5*E*).

Signaling Pathway—The gene name of each differentially expressed protein identified via the database search was imported into Pathway Studio for the determination of a signaling pathway. The schematic image was constructed to determine both physiological function and interactions of identified proteins in spermatozoa. The discovered markers interacted with each other, and were also related to particular cell processes, protein kinases, ligands, complexes, functional classes, and small molecules (Fig. 6).

DISCUSSION

Evaluation of semen quality is very significant step before selection of breeding male used for AI. In fact, the selection of quality semen mainly depends on conventional semen analyses (9–12), but the clinical value of these analyses is still debated (13). Consistent with these findings our data indicated a non-significant difference of motility, motion kinematics, and capacitation status between high- and low-litter size spermatozoa (Table I). Therefore, to evaluate the limits of

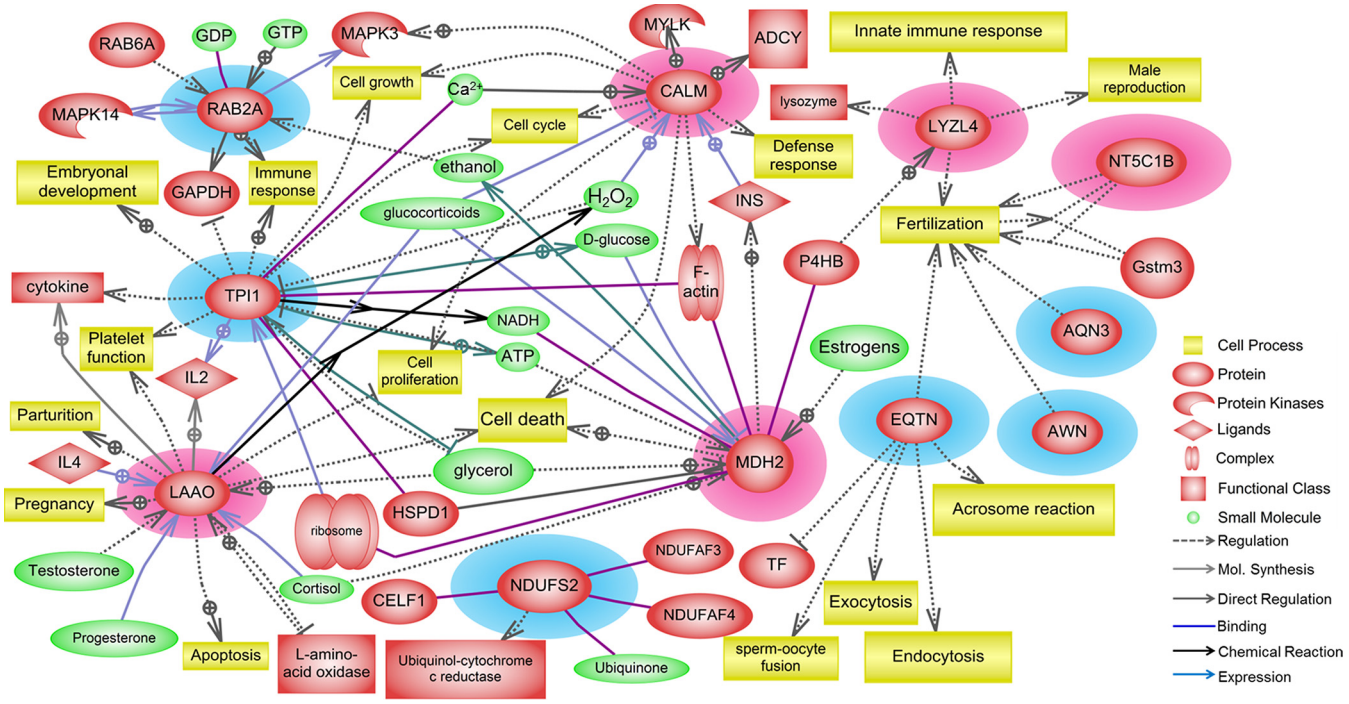

FIG. 6. **Signaling pathways associated with litter size in boars.** The schematic was developed using Pathway Studio 9.0 following a database search in PubMed. Red highlighted proteins were abundantly expressed in high-litter size spermatozoa, and blue highlighted proteins were abundantly expressed in low-litter size spermatozoa.

conventional semen analyses, the development of new methods to assess sperm function and male fertility should be considered seriously. Recent proteomic tools have identified several proteins associated with fertility or infertility of animals and humans (4, 18). Concurrently, several attempts also have been undertaken to identify differentially expressed proteins in spermatozoa to address these issues more precisely in mammals (17, 27, 28). However, it is always arguable whether a single criterion (*e.g.* fertile *versus* non-fertile, high *versus* low fertility, high- *versus* low-litter size, etc.) can accurately represent the state of fertility. Therefore, to discover predictive biomarkers for male fertility, we applied a comprehensive proteomic approach to evaluate changes of global protein profiles between high- and low-litter sizes in boar spermatozoa.

In present study, 11 significant differentially expressed proteins were detected between high- and low-litter size spermatozoa using PDQuest 8.0, ESI-MS/MS, and a MASCOT search (>threefold, Fig. 2 and 3). Among these proteins, EQTN, AWN, TPI, RAB2A, AQN-3, and NDUFS2 were significantly and abundantly expressed in low-litter size spermatozoa (>threefold, $p < 0.05$, Fig. 3*A*). The literature demonstrates that EQTN, a complex 38–48 kDa protein, is located in the equatorial and acrosomal region in mammalian species (29–31). Furthermore, EQTN is preserved in the equatorial segment and exposed after acrosome reaction to facilitate sperm-oocyte interaction and fertilization (30–32). Recent studies have demonstrated that *Eqtn* knockout mouse ($Eqtn^{-/-}$) spermatozoa have a deficiency in acrosome reaction and fertilization, but they have normal motility and morphology (33). These results indicate that EQTN may play a key role in acrosome reaction and sperm-oocyte interaction. RAB2A is one of the important proteins in acrosome formation in spermatozoa, and it is a subgroup of the RAB family, which has a critical role in regulating vesicular transport and membrane fusion. RAB2A is located in the acrosome membrane of spermatozoa (34, 35). Therefore, RAB2A is involved in the structural modification of the acrosome to induce acrosome reaction following capacitation (36, 37). Both AQN-3 and AWN have been identified in low-molecular mass in boar spermatozoa (38, 39). The proteins represent ZP-binding proteins, which have 109–133 amino acids and two disulfide bonds (40). Previous studies have shown that high amounts of these proteins coat the sperm surface after ejaculation, and are released after capacitation (41). These proteins play a key role in capacitation and gamete recognition (41). Therefore, the differential expression of EQTN, RAB2A, AQN-3, and AWN supports the potential involvement of these proteins in the regulation of male fertility by acrosome reaction and sperm-egg interaction.

Other proteins that are significantly and abundantly expressed in low-litter size spermatozoa were NDUFS2 and TPI (>threefold, $p < 0.05$, Fig. 3*A*). NDUFS2 is a known NADH-ubiquinone oxidoreductase 49 kDa subunit (42, 43). NADH dehydrogenase contributes to site I of the mitochondrial electron transport chain (44). In spermatozoa, NADH dehydrogen-

ase is closely involved in tyrosine phosphorylation and sperm motility (44–46). TPI stimulates the reversible interconversion of the triose phosphate isomers dihydroxyacetone phosphate and d-glyceraldehyde 3-phosphate in the glycolysis pathway (47). Moreover, TPI is an essential enzyme in glucose metabolism that is required to initiate capacitation and the acrosome reaction via the contribution of ATP that is gained through the breakdown of glucose (47). Recent studies have shown that levels of TPI were higher in asthenozoospermic samples than normospermic samples; in addition, higher levels of TPI have been identified in poor freezability samples compared with the good freezability samples (48, 49). These results suggest that high levels of TPI in spermatozoa have an adverse effect on motility and male fertility. Interestingly, TPI was abundantly expressed in low-litter size, while no significant difference in motility was detected between high- and low-litter size spermatozoa in the present study. This may suggest that TPI plays a critical role during capacitation. Therefore, the differential expression of NDUFS2 and TPI support their potential involvement in regulating male fertility.

Among the 11 proteins, five (LAAO, MDH2, NT5C1B, LYZL4, and CALM) were significantly and abundantly expressed in low-litter size spermatozoa as compared with high-litter size spermatozoa in 2-DE analyses (>3-fold; $p < 0.05$; Fig. 3*B*). LAAO is a well-known enantioselective flavoenzyme that catalyzes the stereospecific oxidative deamination of l-amino acids to α-keto acids, ammonia, and hydrogen peroxide (50). LAAO is a potential enzyme that is active after sperm cell death. To activate LAAO, the permeability of the membrane related to cell senescence and death is increased (51, 52). Shannon and Curson (51) reported that LAAO is located in the bovine sperm tail. However, further research is needed to elucidate the effect of LAAO on spermatozoa.

MDH is a key protein in cellular respiration, and it is a distinguished isoenzyme depending on its location: cytosolic (MDH-NADP) or mitochondrial (MDH-NAD) (52, 53). MDH-NAD is located in the mid-piece of mammalian spermatozoa (ram, boar, and buffalo) (53, 54). Recent studies have shown that MDH contributes to capacitation and acrosome reaction in cryopreserved bovine spermatozoa (54). In the present study, MDH was differentially expressed according to litter size. Therefore, differential expression of MDH supports its potential involvement in regulating male fertility by facilitating capacitation and acrosome reaction. 5′-nucleotidases are known to regulate nucleotide and nucleoside levels in the cell by catalysis of transfer or hydrolysis of esterified phosphates at the 5′ position of nucleoside monophosphates (55–57). Previous studies have reported that 5′-nucleotidase is located in the outer leaflet of the plasma membrane in spermatozoa (58, 59). Schiemann *et al.* (58) reported that endogenous 5′-nucleotidase is present at the postacrosome region in bovine spermatozoa, and it provides specialized functions during the acrosome reaction. Other studies suggested that ecto-5′-nucleotidase plays a role in the regulation of sperm motility such as the decrease in sperm motility after freezing (59, 60). Chicken-type (c-type) lysozyme consists of four genes (*Lyzl2, Lyzl4, Lyzl6, and Spaca3*) (61, 62). Particularly, LYZL4 is located in the acrosome region and is a principle component of spermatozoa (62, 63). Recent studies reported that the inhibition of LYZL4 with its specific antibody in spermatozoa led to decreased fertilizing ability (64). Therefore, LYZL4 may play a key role in fertilization processes that control motility and the acrosome reaction in spermatozoa (62, 63). CALM is a multifunctional intermediate messenger protein that modifies interactions between various target proteins by binding calcium ions (64, 65). Previous studies reported that CALM is located in the acrosome region and flagellum in spermatozoa (66–68). These studies suggest that CALM is essential to the acrosome reaction and motility (66, 68). Therefore, the differential expression of MDH, NT5C1B, LYZL4, and CALM suggest their potential involvement in male fertility regulation. It is important to note that, the expression levels of MDH2 and CALM between high- and low-litter size spermatozoa were >5-fold in 2-DE, whereas they were only ~twofold in Western blot (Fig. 3 and 4). Perhaps the most straightforward explanation of these discrepancies was due to use of silver staining, as this staining represents several inherent limitations and incapable to provide adequate quantitation of low-abundance proteins (69–72). In order to compensate this weakness, additional validation of 2-DE results is strongly recommended when the silver staining used. Therefore, Western blot and individual ELISA analysis were performed in the study.

In present study, RAB2A, TPI, and NDUFS2 were negatively correlated with litter size ($p < 0.01$, Table III), while CALM and MDH2 were positively correlated with litter size ($p < 0.01$, Table III). The overall accuracy of the assay for the prediction of litter sizes using the expression levels of RAB2A, TPI, NDUFS2, CALM, and MDH2 were 70.00%, 60.00%, 70.00%, 85.00%, and 80.00%, respectively (Table IV). These predictive values of novel protein markers were lower than our expectations. However the average litter size following protein expression levels based on cut-off values for litters of 11 was significantly increased by ~0.8 pups in AI field trials (Fig. 5). One of the purposes of this study was to understand the function of the proteins that had changed their abundance between high- and low-litter size spermatozoa. To gain a better understanding of these 11 proteins, we established a new signaling pathway that interacted with each other and those associated with particular cell processes, protein kinases, ligands, complexes, functional classes, and small molecules. Additionally, differentially expressed proteins potentially regulate male fertility via interaction of proteins and their associated signaling cascades, which collectively aid the metabolism of spermatozoa (Fig. 6).

To the best of our knowledge, this is the first work that utilized male fertility biomarkers to predict litter size in a field trial. We discovered 11 biomarkers and provided evidence that these markers are acceptable predictors of porcine male

fertility. The biomarkers may be particularly important in the animal industry for the prediction and selection of superior sires. If it is possible to increase 2 pups/year by applying currently discovered markers, it will contribute hugely in subsequent breeding. Therefore, one can easily speculate the importance of these markers' economic impact. These protein markers may also provide clues to aid our understanding of sperm function as well as mechanisms of fertilization. Furthermore, the biomarkers are also potential candidates for male contraceptive targeting. We believe that our findings may be answered the fertility questions more precisely from a proteomic point of view.

* This work was supported by a grant from the Next-Generation BioGreen 21 Program (No. PJ01106101), Rural Development Administration, Republic of Korea.

§ To whom correspondence should be addressed: Chung-Ang University, Anseong, Gyeonggi-Do 456-756, Republic of Korea. Tel.: +82.31.670.4841; Fax: +82.31.675.9001; E-mail: mgpang@cau.ac.kr.

REFERENCES

1. Kwon, W. S., Rahman, M. S., and Pang, M. G. (2014) Diagnosis and Prognosis of Male Infertility in Mammal: The Focusing of Tyrosine Phosphorylation and Phosphotyrosine Proteins. *J. Proteome Res.* **13,** 4505–4517
2. Sharlip, I. D., Jarow, J. P., Belker, A. M., Lipshultz, L. I., Sigman, M., Thomas, A. J., Schlegel, P. N., Howards, S. S., Nehra, A., Damewood, M. D., Overstreet, J. W., and Sadovsky, R. (2002) Best practice policies for male infertility. *Fertil.. Steril.* **77,** 873–882
3. Peddinti, D., Nanduri, B., Kaya, A., Feugang, J. M., Burgess, S. C., and Memili, E. (2008) Comprehensive proteomic analysis of bovine spermatozoa of varying fertility rates and identification of biomarkers associated with fertility. *BMC Syst. Biol.* **2,** 19
4. Park, Y. J., Kwon, W. S., Oh, S. A., and Pang, M. G. (2012) Fertility-related proteomic profiling bull spermatozoa separated by percoll. *J. Proteome Res.* **11,** 4162–4168
5. Park, Y. J., Kim, J., You, Y. A., and Pang, M. G. (2013) Proteomic revolution to improve tools for evaluating male fertility in animals. *J. Proteome Res.* **12,** 4738–4747
6. Gerrits, R. J., Lunney, J. K., Johnson, L. A., Pursel, V. G., Kraeling, R. R., Rohrer, G. A., and Dobrinsky, J. R. (2005) Perspectives for artificial insemination and genomics to improve global swine populations. *Theriogenology* **63,** 283–299
7. Dyck, M. K., Foxcroft, G. R., Novak, S., Ruiz-Sanchez, A., Patterson, J., and Dixon, W. T. (2011) Biological markers of boar fertility. *Reprod. Domest. Anim.* **46,** 55–58
8. Gadea, J. (2005) Sperm factors related to in vitro and in vivo porcine fertility. *Theriogenology* **63,** 431–444
9. Bonde, J. P., Ernst, E., Jensen, T. K., Hjollund, N. H., Kolstad, H., Henriksen, T. B., Scheike, T., Giwercman, A., Olsen, J., and Skakkebaek, N. E. (1998) Relation between semen quality and fertility: a population-based study of 430 first-pregnancy planners. *Lancet* **352,** 1172–1177
10. Budworth, P. R., Amann, R. P., and Chapman, P. L. (1988) Relationships between computerized measurements of motion of frozen-thawed bull spermatozoa and fertility. *J. Androl.* **9,** 41–54
11. Oh, S. A., Park, Y. J., You, Y. A., Mohamed, E. A., and Pang, M. G. (2010) Capacitation status of stored boar spermatozoa is related to litter size of sows. *Anim. Reprod. Sci.* **121,** 131–138
12. Oh, S. A., You, Y. A., Park, Y. J., and Pang, M. G. (2010) The sperm penetration assay predicts the litter size in pigs. *Int. J. Androl.* **33,** 604–612
13. Lewis, S. E. (2007) Is sperm evaluation useful in predicting human fertility? *Reproduction* **134,** 31–40
14. Corner, J. S., Barratt, C. L. R. (2006) *Genomic and proteomic approaches to defineing sperm.* In *The sperm cell*, eds De Jonge, C. J., Barratt, C. L. R. pp 49–71. Cambridge University Press, Cambridge, U. K.
15. de Mateo, S., Martínez-Heredia, J., Estanyol, J. M., Domínguez-Fandos, D., Vidal-Taboada, J. M., Ballescà, J. L., and Oliva, R. (2007) Marked correlations in protein expression identified by proteomic analysis of human spermatozoa. *Proteomics* **7,** 4264–4277
16. Kwon, W. S., Rahman, M. S., Lee, J. S., Kim, J., Yoon, S. J., Park, Y. J., You, Y. A., Hwang, S., and Pang, M. G. (2014) A comprehensive proteomic approach to identifying capacitation related proteins in boar spermatozoa. *BMC Genomics.* **14,** 897
17. Baker, M. A., Reeves, G., Hetherington, L., and Aitken, R. J. (2010) Analysis of proteomic changes associated with sperm capacitation through the combined use of IPG-strip pre-fractionation followed by RP chromatography LC-MS/MS analysis. *Proteomics* **10,** 482–495
18. Oliva, R., de Mateo, S., and Estanyol, J. M. (2009) Sperm cell proteomics. *Proteomics* **9,** 1004–1017
19. Almond, G., Britt, J., Flowers, B., Glossop, C., Levis, D., Morrow, M., and See, T. (1998) The Swine A. I. Book, Morgan Morrow Press, Raleigh, NC.
20. Schulze, M., Ruediger, K., Mueller, K., Jung, M., Well, C., and Reissmann, M. (2013) Development of an in vitro index to characterize fertilizing capacity of boar ejaculates. *Anim. Reprod. Sci.* **140,** 70–76
21. Flesch, F. M., Colenbrander, B., van Golde, L. M., and Gadella, B. M. (1999) Capacitation induces tyrosine phosphorylation of proteins in the boar sperm plasma membrane. *Biochem. Biophys. Res. Commun.* **262,** 787–792
22. Kwon, W. S., Park, Y. J., Kim, Y. H., You, Y. A., Kim, I. C., and Pang, M. G. (2013) Vasopressin effectively suppresses male fertility. *PLoS ONE* **8,** e54192
23. Kwon, W. S., Park, Y. J., Mohamed, el-S. A., and Pang, M. G. (2013) Voltage-dependent anion channels are a key factor of male fertility. *Fertil. Steril.* **99,** 354–361
24. Rahman, M. S., Kwon, W. S., Lee, J. S., Kim, J., Yoon, S. J., Park, Y. J., You, Y. A., Hwang, S., and Pang, M. G. (2014) Sodium nitroprusside suppresses male fertility in vitro. *Andrology* **2,** 899–909
25. Mohamed, el-S. A., Park, Y. J., Song, W. H., Shin, D. H., You, Y. A., Ryu, B. Y., and Pang, M. G. (2011) Xenoestrogenic compounds promote capacitation and an acrosome reaction in porcine sperm. *Theriogenology* **75,** 1161–1169
26. Park, Y. J., Mohamed, el-S. A., Oh, S. A., Yoon, S. J., Kwon, W. S., Kim, H. R., Lee, M. S., Lee, K., and Pang, M. G. (2012) Sperm penetration assay as an indicator of bull fertility. *J. Reprod. Dev.* **58,** 461–466
27. Jagan Mohanarao, G., and Atreja, S. K. (2011) Identification of capacitation associated tyrosine phosphoproteins in buffalo (Bubalus bubalis) and cattle spermatozoa. *Anim. Reprod. Sci.* **123,** 40–47
28. Secciani, F., Bianchi, L., Ermini, L., Cianti, R., Armini, A., La Sala, G. B., Focarelli, R., Bini, L., and Rosati, F. (2009) Protein profile of capacitated versus ejaculated human sperm. *J. Proteome Res.* **8,** 3377–3389
29. Toshimori, K., Tanii, I., Araki, S., and Oura, C. (1992) Characterization of the antigen recognized by a monoclonal antibody MN9: unique transport pathway to the equatorial segment of sperm head during spermiogenesis. *Cell Tissue Res.* **270,** 459–468
30. Toshimori, K., Saxena, D. K., Tanii, I., and Yoshinaga, K. (1998) An MN9 antigenic molecule, equatorin, is required for successful sperm-oocyte fusion in mice. *Biol. Reprod.* **59,** 22–29
31. Yoshinaga, K., Saxena, D. K., Oh-oka, T., Tanii, I., and Toshimori, K. (2001) Inhibition of mouse fertilization in vivo by intra-oviductal injection of an anti-equatorin monoclonal antibody. *Reproduction* **122,** 649–655
32. Hao, J., Chen, M., Ji, S., Wang, X., Wang, Y., Huang, X., Yang, L., Wang, Y., Cui, X., Lv, L., Liu, Y., and Gao, F. (2014) Equatorin is not essential for acrosome biogenesis but is required for the acrosome reaction. *Biochem. Biophys. Res. Commun.* **444,** 537–542
33. Manandhar, G., and Toshimori, K. (2001) Exposure of sperm head equatorin after acrosome reaction and its fate after fertilization in mice. *Biol. Reprod.* **65,** 1425–1436
34. Mountjoy, J. R., Xu, W., McLeod, D., Hyndman, D., and Oko, R. (2008) RAB2A: a major subacrosomal protein of bovine spermatozoa implicated in acrosomal biogenesis. *Biol. Reprod.* **79,** 223–232
35. Oko, R., and Sutovsky, P. (2009) Biogenesis of sperm perinuclear theca and its role in sperm functional competence and fertilization. *J. Reprod. Immunol.* **83,** 2–7
36. Rahman, M. S., Lee, J. S., Kwon, W. S., and Pang, M. G. Sperm proteomics: Road to male fertility and contraception. *Int. J. Endocrinol.* 2013:

360986, 2013
37. Wu, L., and Sampson, N. S. (2014) Fucose, mannose, and β-N-acetylglucosamine glycopolymers initiate the mouse sperm acrosome reaction through convergent signaling pathways. *ACS Chem. Biol.* **9,** 468–475
38. Sanz, L., Calvete, J. J., Mann, K., Schäfer, W., Schmid, E. R., and Töpfer-Petersen, E. (1991) The amino acid sequence of AQN-3, a carbohydrate-binding protein isolated from boar sperm. Location of disulphide bridges. *FEBS Lett.* **291,** 33–36
39. Sanz, L., Calvete, J. J., Mann, K., Schäfer, W., Schmid, E. R., Amselgruber, W., Sinowatz, F., Ehrhard, M., and Töpfer-Petersen, E. (1992) The complete primary structure of the spermadhesin AWN, a zona pellucida-binding protein isolated from boar spermatozoa. *FEBS Lett.* **300,** 213–218
40. Calvete, J. J., Solís, D., Sanz, L., Díaz-Mauriño, T., Schäfer, W., Mann, K., and Töpfer-Petersen, E. (1993) Characterization of two glycosylated boar spermadhesins. *Eur. J. Biochem.* **218,** 719–725
41. Dostàlovà, Z., Calvete, J. J., Sanz, L., and Töpfer-Petersen, E. (1994) Quantitation of boar spermadhesins in accessory sex gland fluids and on the surface of epididymal, ejaculated and capacitated spermatozoa. *Biochim. Biophys. Acta* **1200,** 48–54
42. Fearnley, I. M., Finel, M., Skehel, J. M., and Walker, J. E. (1991) NADH: ubiquinone oxidoreductase from bovine heart mitochondria. cDNA sequences of the import precursors of the nuclear-encoded 39 kDa and 42 kDa subunits. *Biochem. J.* **278**(Pt 3), 821–829
43. Procaccio, V., de Sury, R., Martinez, P., Depetris, D., Rabilloud, T., Soularue, P., Lunardi, J., and Issartel, J. (1998) Mapping to 1q23 of the human gene (NDUFS2) encoding the 49-kDa subunit of the mitochondrial respiratory Complex I and immunodetection of the mature protein in mitochondria. *Mamm. Genome* **9,** 482–484
44. Ruiz-Pesini, E., Diez, C., Lapeña, A. C., Pérez-Martos, A., Montoya, J., Alvarez, E., Arenas, J., and López-Pérez, M. J. (1998) Correlation of sperm motility with mitochondrial enzymatic activities. *Clin. Chem.* **44,** 1616–1620
45. Arcelay, E., Salicioni, A. M., Wertheimer, E., and Visconti, P. E. (2008) Identification of proteins undergoing tyrosine phosphorylation during mouse sperm capacitation. *Int. J. Dev. Biol.* **52,** 463–472
46. Loza-Huerta, A., Vera-Estrella, R., Darszon, A., and Beltrán, C. (2013) Certain Strongylocentrotus purpuratus sperm mitochondrial proteins co-purify with low density detergent-insoluble membranes and are PKA or PKC-substrates possibly involved in sperm motility regulation. *Biochim. Biophys. Acta* **1830,** 5305–5315
47. Fraser, L. R., and Quinn, P. J. (1981) A glycolytic product is obligatory for initiation of the sperm acrosome reaction and whiplash motility required for fertilization in the mouse. *J. Reprod. Fertil.* **61,** 25–35
48. Siva, A. B., Kameshwari, D. B., Singh, V., Pavani, K., Sundaram, C. S., Rangaraj, N., Deenadayal, M., and Shivaji, S. (2010) Proteomics-based study on asthenozoospermia: differential expression of proteasome alpha complex. *Mol. Hum. Reprod.* **16,** 452–462
49. Vilagran, I., Castillo, J., Bonet, S., Sancho, S., Yeste, M., Estanyol, J. M., and Oliva, R. (2013) Acrosin-binding protein (ACRBP) and triosephosphate isomerase (TPI) are good markers to predict boar sperm freezing capacity. *Theriogenology* **80,** 443–450
50. Guo, C., Liu, S., Yao, Y., Zhang, Q., and Sun, M. Z. (2012) Past decade study of snake venom L-amino acid oxidase. *Toxicon* **60,** 302–311
51. Shannon, P., and Curson, B. (1982) Site of aromatic L-amino acid oxidase in dead bovine spermatozoa and determination of between-bull differences in the percentage of dead spermatozoa by oxidase activity. *J. Reprod. Fertil.* **64,** 469–473
52. Shannon, P., and Curson, B. (1982) Kinetics of the aromatic L-amino acid oxidase from dead bovine spermatozoa and the effect of catalase on fertility of diluted bovine semen stored at 5 degrees C and ambient temperatures. *J. Reprod. Fertil.* **64,** 463–467
53. Kohsaka, T., Takahara, H., Tagami, S., Sasada, H., and Masaki, J. (1992) A new technique for the precise location of lactate and malate dehydrogenases in goat, boar and water buffalo spermatozoa using gel incubation film. *J. Reprod. Fertil.* **95,** 201–209
54. Córdoba, M., Pintos, L., and Beconi, M. T. (2005) Differential activities of malate and isocitrate NAD(P)-de pendent dehydrogenases are involved in the induction of capacitation and acrosome reaction in cryopreserved bovine spermatozoa. *Andrologia* **37,** 40–46
55. Hunsucker, S. A., Mitchell, B. S., and Spychala, J. (2005) The 5′-nucleotidases as regulators of nucleotide and drug metabolism. *Pharmacol. Therapeutics* **107,** 1–30
56. Bogan, K. L., and Brenner, C. (2010) 5′-Nucleotidases and their new roles in NAD+ and phosphate metabolism. *New J. Chem.* **34,** 845–853
57. Santos, C. A., Saraiva, A. M., Toledo, M. A., Beloti, L. L., Crucello, A., Favaro, M. T., Horta, M. A., Santiago, A. S., Mendes, J. S., Souza, A. A., and Souza, A. P. (2013) Initial biochemical and functional characterization of a 5′-nucleotidase from Xylella fastidiosa related to the human cytosolic 5′-nucleotidase I. *Microb. Pathog.* **59–60**, 1–6
58. Schiemann, P. J., Aliante, M., Wennemuth, G., Fini, C., and Aumüller, G. (1994) Distribution of endogenous and exogenous 5′-nucleotidase on bovine spermatozoa. *Histochemistry* **101,** 253–262
59. Aumüller, G., Renneberg, H., Schiemann, P. J., Wilhelm, B., Seitz, J., Konrad, L., and Wennemuth, G. (1997) The role of apocrine released proteins in the post-testicular regulation of human sperm function. *Adv. Exp. Med. Biol.* **424,** 193–219
60. Huang, S. Y., Pribenszky, C., Kuo, Y. H., Teng, S. H., Chen, Y. H., Chung, M. T., Chiu, Y. F. (2009) Hydrostatic pressure pre-treatment affects the protein profile of boar sperm before and after freezing-thawing. *Anim. Reprod. Sci.* **112,** 136–149
61. Zhang, K., Gao, R., Zhang, H., Cai, X., Shen, C., Wu, C., Zhao, S., and Yu, L. (2005) Molecular cloning and characterization of three novel lysozyme-like genes, predominantly expressed in the male reproductive system of humans, belonging to the c-type lysozyme/alpha-lactalbumin family. *Biol. Reprod.* **73,** 1064–1071
62. Sun, R., Shen, R., Li, J., Xu, G., Chi, J., Li, L., Ren, J, Wang, Z., and Fei, J. (2011) Lyzl4, a novel mouse sperm-related protein, is involved in fertilization. *Acta Biochim. Biophys. Sin.* **43,** 346–353
63. Narmadha, G., Muneswararao, K., Rajesh, A., and Yenugu, S. (2011) Characterization of a novel lysozyme-like 4 gene in the rat. *PLoS ONE* **6,** e27659
64. Stevens, F. C. (1983) Calmodulin: an introduction. *Can. J. Biochem. Cell Biol.* **61,** 906–910
65. Chin, D., and Means, A. R. Calmodulin (2000) a prototypical calcium sensor. *Trends Cell Biol.* **10,** 322–328
66. Bendahmane, M., Lynch, C 2nd., and Tulsiani, D. R. (2001) Calmodulin signals capacitation and triggers the agonist-induced acrosome reaction in mouse spermatozoa. *Arch Biochem. Biophys.* **390,** 1–8
67. Colás, C., Grasa, P., Casao, A., Gallego, M., Abecia, J. A., Forcada, F., Cebrián-Pérez, J. A., and Muiño-Blanco, T. (2009) Changes in calmodulin immunocytochemical localization associated with capacitation and acrosomal exocytosis of ram spermatozoa. *Theriogenology* **71,** 789–800
68. Lasko, J., Schlingmann, K., Klocke, A., Mengel, G. A., and Turner, R. (2012) Calcium/calmodulin and cAMP/protein kinase-A pathways regulate sperm motility in the stallion. *Anim. Reprod. Sci.* **132,** 169–177
69. Li, Z. B., Flint, P. W., and Boluyt, M. O. (2005) Evaluation of several two-dimensional gel electrophoresis techniques in cardiac proteomics. *Electrophoresis* **26,** 3572–3585
70. White, I. R., Pickford, R., Wood, J., Skehel, J. M., Gangadharan, B., and Cutler, P. (2004) A statistical comparison of silver and SYPRO Ruby staining for proteomic analysis. *Electrophoresis* **25,** 3048–3054
71. Smales, C. M., Birch, J. R., Racher, A. J., Marshall, C. T., and James, D. C. (2003) Evaluation of individual protein errors in silver-stained two-dimensional gels. *Biochem. Biophys. Res. Commun.* **306,** 1050–1055
72. Shaw, J., Rowlinson, R., Nickson, J., Stone, T., Sweet, A., Williams, K., and Tonge, R. (2003) Evaluation of saturation labelling two-dimensional difference gel electrophoresis fluorescent dyes. *Proteomics* **3,** 1181–1195